Interconnect Reliability Modeling and Analysis for Multi-Branch Interconnect Trees

Hai-Bao Chen*, Sheldon X.-D. Tan†, Valeriy Sukharev ‡, Xin Huang† and Taeyoung Kim§
* Department of Micro/Nano-electronics, Shanghai Jiao Tong University, Shanghai 200240, China
† Department of Electrical and Computer Engineering, University of California, Riverside, CA 92521, USA
‡ Mentor Graphics Corporation, Fremont, CA 94538, USA
§ Department of Computer Science and Engineering, University of California, Riverside, CA 92521, USA

***Abstract*—Electromigration (EM) in VLSI interconnects has become one of the major reliability issues for current and future VLSI technologies. However, existing EM modeling and analysis techniques are mainly developed for a single wire. For practical VLSI chips, the interconnects such as clock and power grid networks typically consist of multi-branch metal segments representing a continuously connected, highly conductive metal (Cu) lines within one layer of metallization, terminating at diffusion barriers. The EM effects in those branches are not independent and they have to be considered simultaneously. In this paper, we demonstrate, for the first time, a first principle based analytic solution of this problem. We investigate the analytic expressions describing the hydrostatic stress evolution in several typical interconnect trees: the straight-line 3-terminal wires, the T-shaped 4-terminal wires and the cross-shaped 5-terminal wires. The new approach solves the stress evolution in a multi-branch tree by de-coupling the individual segments through the proper boundary conditions accounting the interactions between different branches. By using Laplace transformation technique, analytical solutions are obtained for each type of the interconnect trees. The analytical solutions in terms of a set of auxiliary basis functions using the complementary error function agree well with the numerical analysis results. Our analysis further demonstrates that using the first two dominant basis functions can lead to 0.5% error, which is sufficient for practical EM analysis.**

I. Introduction

Electromigration-induced reliability becomes a major design constraint in the current and future nanometer VLSI technologies. To ensure the EM signoff, conservative design rules based on the worst cases (highest possible temperature and power consumption) and simple EM model such as Black's equation can lead to significant overdesign and 2X-3X enlarged guard bands [1]. Such conservative and overdesign rules, however, will be no longer an option in current and future technologies because 3X guard band increase will significantly increase the buffer size and many other aspects of chips, which will lead to increasing currents, thus costs and powers of the chips. As a result, more accurate EM modeling and analysis techniques are required to ensure sufficient accuracy without hurting the efficiencies.

Existing EM model and analysis techniques mainly focus on the simple straight line interconnect with two-line end terminals. However, a practical integrated circuit layout often has interconnects such as clock and power grid networks with more complex structures. The EM effects in those branches are not independent and they have to be considered simultaneously [2] [3]. Currently employed Blech limit [4] (for the out filtration of immortal segments) and Black's equation [5] (for calculating MTTFs for segments characterized by known current densities and temperatures) are subjects of the hard criticism [6] [7] [8]. Across-die variation of residual stress makes the Blech's "critical product" to be layout-dependent variables rather than experimentally determined constants. Interdependency of the Black's activation energy and current density exponent on the current density and temperature makes rather controversial the widely accepted methodology of calculating the MTTF at use condition, represented by chip operation current density and temperature, while using the activation energy and current density exponent determined at the stressed (accelerated) condition, characterized by high current densities and elevated temperatures.

Recently some physics-based EM analysis methods for the TSV and power grid networks have been proposed based on solving the basic mass transport equations [9]. Those models treat the resistance changes of a wire over time as the atomic concentration changes due to atomic flux. Since these proposed methods solve the basic mass transport equations using the finite element method, they can only solve for very small structures such as one TSV structure. Complicated look-up table or models have to be built for different TSVs and wire segments for full-chip power grid analysis at reduced accuracy. To mitigate this problem, a more compact physics-based EM model was proposed recently in [10] [11]. It is based on the hydrostatic stress diffusion equation [12]. Although the new EM model has been extended to deal with multiple branch tree wire based on projected steady-state stress. It still can't provide the time-dependent hydrostatic evolution of hydrostatic stress, which ultimately determines the failures for multi-branch interconnect wires.

To further illustrate this, Fig. 1 shows distributions of the current density and hydrostatic stress developed in the three terminals interconnect tree [10]. Two vias are used as the electron flow inlets and one positively biased as outlet. The hydrostatic stress obtained from the solution of the system of

This work is supported in part by NSF grant under No. CCF-1017090, in part by NSF Grant under No. CCF-1255899, in part by Semiconductor Research Corporation (SRC) grant under No. 2013-TJ-2417, in part by a 985 research fund from Shanghai Jiao Tong University, in part by NSFC grant under No. 20873999.

DAC'15, June 07-11,2015,San Francisco,CA,USA Copyright 2015 ACM 978-1-4503-3520-1/15/06$15.00 http://dx.doi.org/10.1145/2744769.2747953

partial differential equations with the FEA tool COMSOL [13] demonstrates the two-slope distribution resulted by the intra branch atom diffusion. It is clear that this stress distribution can be explained by redistribution of the atoms among both the branches of the tree. Tree decomposition on two independent segments will never explain this type of stress distribution [14]. Closed-form analytical description of the distribution of hydrostatic stress caused by EM-induced redistribution of atoms inside an interconnect tree, which is needed for determination of the potential locations for void nucleation, is the major motivation for the proposed work.

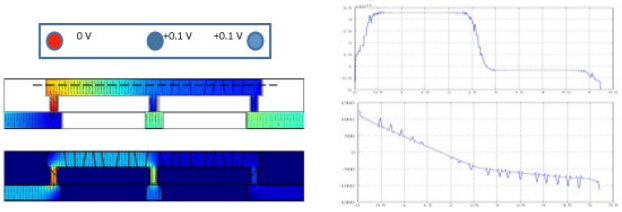

(a) (b)

Fig. 1. Hydrostatic stress (a) and current density (b) distributions along the top metal line.

A. Related works

Many existing works have been proposed to study the multi-branch interconnects in the past and most of them focus on experimental characterizations, instead of compact modeling. Vairagar ***et al.*** studied the dependence of EM-induced failure in a 3-terminal single wire in a Cu interconnect tree on the electric current configuration in adjoining interconnect segments and provided direct evidence of the peculiar EM behavior based on the proposed EM failure mechanism [15]. Experimental characterization of the reliability of dual-damascene Cu interconnect tree structures consisting of straight contact-to-contact lines has been analyzed in [16]–[18]. However, it did not give a unified analytic form to model the 3-terminal interconnect trees which strongly depend on the stress evolution of neighboring segments. In [19], the effects of EM in a 3-terminal L-shaped interconnect tree were simulated by using a numerical simulator based on the solution of one-dimensional Korhonen equation. An analytic model for the evolution in the star-like tree represented by semi-infinite segments with known current densities connected at the central node has been developed [14] [20]. In order to implement critical threshold design rules of EM reliability, a nodal analysis technique for computing the steady-state EM-induced stress was proposed in [21]. The nodal analysis technique is an approximate method for calculating the node voltages at the end of the interconnect segments extracted from the larger interconnect network.

In this work, we propose, for the first time, an accurate and first principle based analytic model for calculating the hydrostatic stress evolution in the finite multi-branch interconnect trees during the void nucleation phase. We have derived the analytic expressions describing the hydrostatic stress evolution in several typical interconnect trees: the straight-line 3-terminal wires, the T-shaped 3-terminal wires and the cross-shaped 4-terminal wires. This new approach solves the stress evolution in a multi-branch tree by de-coupling the individual segments through the proper boundary conditions accounting the interactions between different branches. By using Laplace transformation technique, analytical solutions are obtained for each tree. The analytical solutions then are obtained in terms of set of auxiliary basis functions using the complementary error function. Those analytical EM models agree well with COMSOL simulation results. Furthermore, we demonstrates that employing the first dominant basis function can lead to less than 4 % errors and by using the first two basis functions, one can have less than 0.5% errors, which is sufficient for practical EM analysis.

II. The Dynamic Stress Evaluation for a Single Segment Wire

Before we present our analytic solutions for multi-branch interconnect trees. Let us review the basic equation describing the hydrostatic stress in a single segment wire with blocking boundary conditions (BC).

For a one dimensional metal wire, the stress evolution $\sigma(t)$ caused by EM effects is well described by the following diffusion-like equation [12]:

$$\frac{\partial \sigma(x,t)}{\partial t} = \frac{\partial}{\partial x}[\kappa(\frac{\partial \sigma(x,t)}{\partial x} + G)], \tag{1}$$

where $\kappa = \frac{D_a B \Omega}{kT}$ is the "stress" diffusivity and $G = \frac{Eq^*}{\Omega}$ is the EM driving force, D_a is the effective atomic diffusion coefficient,

$$D_a = D_0 \exp(-\frac{E_a}{kT}). \tag{2}$$

Here, D_0 is the pre-exponential factor, E_a is the activation energy, B is the effective bulk modulus, Ω is the atomic volume, k is Boltzmann's constant, T is the absolute temperature, E is the electric field, and q^* is the effective charge. The electric field E can be replaced by the product of the resistivity ρ times the current density j, i.e., $E = \rho j$. The effective charge $q^* = |Z^*|e$ is a known quantity, where e is the elementary charge and Z^* is the effective charge number. As a result, driving force G can be re-written as $G = \frac{\rho j |Z^*| e}{\Omega}$. To facilitate the comprehension of this paper, we summarize the major notations in Table I.

Fig. 2 shows the stress development over time in a metal line computed by COMSOL [13]. Over time, tensile (the positive)

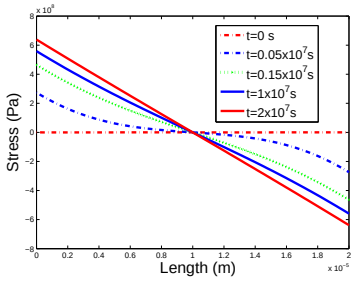

Fig. 2. The EM-induced stress development and distribution in a single metal wire

stress will be developed at the cathode node (left node) and compressive (negative) stress will be developed at the anode (right) node. The stress changes sign in the middle of the wire.

TABLE I
NOTATIONS AND TYPICAL VALUE IN OUR TRANSIENT SIMULATION

Term	Typical value	Description
ρ	1.67e-8$\Omega\cdot$ m	Electrical resistivity
e	1.60e-19C	Electric charge
Z^*	10	Effective valence charge
Ω	8.78e-30 m^3	Atomic volume
k	1.38e-23J/K	Boltzmann constant
B	1e11Pa	Back flow stress modular
D_0	7.56e-5m^2/ s	Self-diffusion coefficient
E_a	0.8eV	Activation energy
σ_T	400MPa	Thermal stress
j	From simulation	Current density
T	From simulation	Absolute temperature
σ	From simulation	Electromigration stress

The built-up stress (its gradient) will serve as the counter-force for atomic flux. If the largest stress at the cathode node exceeds critical stress (not shown in the figure), then voids will be created. If the stress development enter a steady state (atomic diffusion stops) before it reaches the critical stress, the wire will become immortal.

Eq. (1) can have a closed-form solution with some boundary conditions. We first assume that the diffusivity κ is not the function of time. For the blocking BC, the flux of stress is blocked at both ends $x = 0$ and $x = L$, i.e., $J(0,t) = J(L,t) = 0$ where $J(x,t) = \frac{D_a}{kT}(\frac{d\sigma(x,t)}{dx} + G)$.

The stress evolution in the line can be given as follows [12]

$$\sigma(x,t,\kappa,G) = \sigma_T + GL\{\frac{1}{2} - \frac{x}{L} - 4\sum_{n=0}^{\infty}\frac{\cos((2n+1)\pi\frac{x}{L})}{(2n+1)^2\pi^2\exp((2n+1)^2\pi^2\frac{\kappa t}{L^2})}\}, \quad (3)$$

where σ_T is the pre-existing residual stress due to a thermal process. In the existing EM modeling methods, where interest focuses on finding the void nucleation time when the stress developed in the line has reached the critical stress [21]. To derive the closed-form expression, one can keep the slowest decaying term of the infinite series in (3) to obtain the approximate estimation for stress at the line cathode end ($x = 0$) as

$$\sigma(t,T,j) \approx \sigma_T + GL(\frac{1}{2} - \frac{1}{2\exp\{\frac{D_a B\Omega t}{L^2 kT}\}}). \quad (4)$$

As a result, when $\sigma(t,T,j) \geq \sigma_{crit}$, the nucleation time t_{nuc} can be computed in an analytic form as below [10], [11]

$$t_{nuc} = \frac{L^2 kT}{D_a B\Omega}\ln\{\frac{\frac{\rho j|Z^*|eL}{2\Omega}}{\sigma_T + \frac{\rho j|Z^*|eL}{2\Omega} - \sigma_{crit}}\}. \quad (5)$$

III. NEW ANALYTIC MODELS FOR MULTI-BRANCH INTERCONNECT TREE

In this section, we present our analytic solutions to the multi-branch interconnect trees. We discuss three cases in the following: the straight-line 3-terminal wires, the T-shaped 4-terminal wires and the cross-shaped 5-terminal wires as they are commonly seen in many practical VLSI wiring for a single metal layer. In this work, a tree is defined as a unit of continuously connected high conductivity metal lying within one layer of metallization, and terminating at diffusion barriers such as vias or contacts with refractory metal liners. In the general case, trees have more than one terminating branch.

For multi-branch interconnect tree, their EM behavior for nucleation phase and growth phase still governed by Korhonen's equation [12]. But it is very difficult to solve the whole Korhonen's equation for all the branches at the same time. One viable approach is to break the multi-branch of an interconnect tree into a number of simple single-segment wire such that we can apply the Korhonen's equation for each segment. At the boundaries of the two connected wire segments, their stress values must be continues (the same) and the atomic flux is also continuous as well. Note that the current densities at the boundaries may not be continuous. But the currents for every terminal must meet the KCL law.

Fig. 3 shows interconnect structures we are interested: (a) the straight-line 3-terminal (contacts) interconnect tree; (b) the T-shaped 4-terminal metal interconnect tree; (c) the cross-shaped 5-terminal interconnect tree. In this work, we mainly focus on the three cases and derive the exact analytical expressions and approximate expressions for the hydrostatic stress evaluation for the EM void nucleation phase. We will look at the void growth phase in the future.

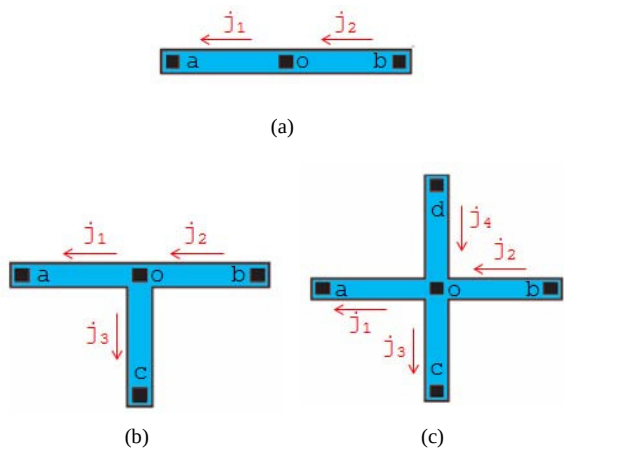

Fig. 3. Interconnect trees for electromigration analysis: (a) the straight-line 3-terminal interconnect tree; (b) the T-shaped 4-terminal interconnect tree; (c) the cross-shaped 5-terminal interconnect tree.

A. Straight-line 3-terminal interconnect tree

We first analyze the 3-terminal interconnect tree with two segments with the current flow directions as showed in Fig. 3(a). The current densities in the two segments may not be the same, which will be determined by the rest of the circuity. For the two segments, we have the following two diffusion equations based on the Korhonen model [12]:

$$\begin{aligned}\frac{\partial\sigma_1(x,t)}{\partial t} &= \frac{\partial}{\partial x}[\kappa_1(\frac{\partial\sigma_1(x,t)}{\partial x} + G_1)], \\ &\quad \texttt{in } -L < x < 0,\ t > 0, \\ \frac{\partial\sigma_2(x,t)}{\partial t} &= \frac{\partial}{\partial x}[\kappa_2(\frac{\partial\sigma_2(x,t)}{\partial x} + G_2)], \\ &\quad \texttt{in } 0 < x < L,\ t > 0.\end{aligned} \quad (6)$$

For the void nucleation phase, the hydrostatic stresses in the two segments will interplay with each other, which is reflected

in the boundary conditions of the following equations:

$$\begin{aligned}
&\kappa_1(\frac{\partial\sigma_1(x,t)}{\partial x}+G_1)=0,\ \texttt{at}\ x=-L,\ t>0,\\
&\sigma_1(x,t)=\sigma_2(x,t),\ \texttt{at}\ x=0,\ t>0,\\
&\kappa_1(\frac{\partial\sigma_1(x,t)}{\partial x}+G_1)=\kappa_2(\frac{\partial\sigma_2(x,t)}{\partial x}+G_2),\\
&\qquad\qquad \texttt{at}\ x=0,\ t>0,\\
&\kappa_2(\frac{\partial\sigma_2(x,t)}{\partial x}+G_2)=0,\ \texttt{at}\ x=L,\ t>0.
\end{aligned} \tag{7}$$

The second equation in (7) means that stresses at the boundary need to be continuous. The third one indicates that the atom flux is also continues at the boundary. The initial conditions of the equations are as follows:

$$\begin{aligned}
&\sigma_1(x,t)=0,\ \texttt{for}\ t=0,\texttt{in}\ -L<x<0,\\
&\sigma_2(x,t)=0,\ \texttt{for}\ t=0,\texttt{in}\ 0<x<L,
\end{aligned} \tag{8}$$

which basically says that there is no stress any where in the whole tree at $t=0$. With the given boundary and initial conditions, it turns out that we can obtain the exact analytical solution for the stresses of the two segments, which is infinite series of some basis functions. For lack of space we omit the details.

On the other hand, our study shows that the if we keep the first dominant term ($n=0$), the error is just about 4%. The approximate solutions with only one dominant term for the segments 1 and 2 are:

$$\begin{aligned}
\sigma_{1,I}(x,t)=&\frac{1}{2}\{2G_1g(\xi_1(x,0),t)+(G_2-G_1)g(\xi_2(x,0),t)\\
&-2G_2g(\xi_3(x,0),t)+(G_2-G_1)g(\xi_4(x,0),t)\}\\
&+\frac{1}{2}\{(G_2-G_1)g(\xi_5(x,0),t)-2G_2g(\xi_6(x,0),t)\\
&+(G_2-G_1)g(\xi_7(x,0),t)+2G_1g(\xi_8(x,0),t)\},
\end{aligned}$$

$$\begin{aligned}
\sigma_{2,I}(x,t)=&\frac{1}{2}\{(G_2-G_1)g(\eta_1(x,0),t)+2G_1g(\eta_2(x,0),t)\\
&+(G_2-G_1)g(\eta_3(x,0),t)-2G_2g(\eta_4(x,0),t)\}\\
&+\frac{1}{2}\{-2G_2g(\eta_5(x,0),t)+(G_2-G_1)g(\eta_6(x,0),t)\\
&+2G_1g(\eta_7(x,0),t)+(G_2-G_1)g(\eta_8(x,0),t)\}.
\end{aligned}$$

For reasons of space, we omit the definitions of the function $\xi()$ and $\eta()$. We will develop the concrete derivations into a journal paper.

Fig. 4 shows the stress evolution of the 3-terminal interconnect tree using the above-mentioned one-term approximation. The proposed method matches with the numerical analysis perfectly at every time instance. In this case, the segment 1 (left) in this case is called ***reservoir*** as it has tensile stress and the segment 2 (right) is called ***sink*** [22]. Typically when the current in the sink is zero or small, voids are only nucleated in the reservoir. This is easily to explain in Fig. 4 as tensile stresses are only seen in the reservoir. But when the sink becomes active (with no zero, same directional current), voids can happen in the sink as well. In this case, the stress in some portions of the sink may exceed a given critical stress shown in Fig. 5, which can well explain the experimental observation in [22].

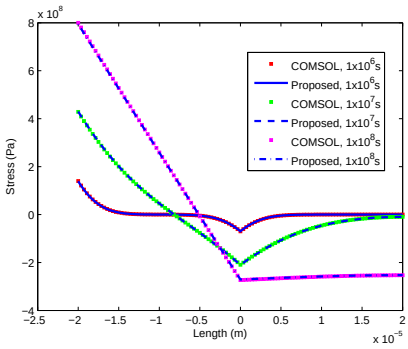

Fig. 4. The EM stress development along the lines 1 and 2 in the 3-terminal single wire interconnect: $j_1=1\times10^{10}A/m^2$, $j_2=0A/m^2$.

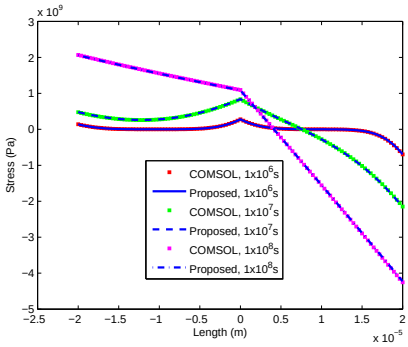

Fig. 5. The EM stress development along the lines 1 and 2 in the 3-terminal single wire interconnect: $j_1=1\times10^{10}A/m^2$, $j_2=5\times10^{10}A/m^2$.

Similar to the single wire case, if we know the critical stress σ_{crit}, which define the stress that void starts to nucleate, then one can compute the void nucleation time t_{nuc} using the new EM model:

$$\begin{aligned}
\sigma_{1,I}(x,t_{nuc,1})&=\sigma_{crit},\\
\sigma_{2,I}(x,t_{nuc,2})&=\sigma_{crit}.
\end{aligned} \tag{9}$$

Since $\sigma_{1,I}(x,t_{nuc,1})$ and $\sigma_{2,I}(x,t_{nuc,2})$ are nonlinear functions, an iterative method will be used to find the t_{nuc}.

B. T-shaped 4-terminal interconnect tree

The structure of the T-shaped 4-terminal interconnect tree has been shown in Fig. 3(b). In this case, we have three segments which connects through the middle contact "o". The stress evolution equation for this interconnect tree consisting of three lines and their exact analytical solutions corresponding to the boundary and initial conditions of the void nucleation phase can also be obtained. Again, we keep the first dominant term as the approximate solution. Due to limited space, we only show the result for the segment 1, $\sigma_{1,T}(x_1,t)$:

$$\begin{aligned}
\sigma_{1,T}(x_1,t)=&-\frac{1}{3}\{-3G_1g(\xi_1(x_1,0),t)+(G_1-G_2\\
&+G_3)g(\xi_2(x_1,0),t)+(G_1+2G_2-2G_3)g(\xi_3(x_1,0),t)\\
&+(G_1-G_2+G_3)g(\xi_4(x_1,0),t)\}-\frac{1}{3}\{(G_1-G_2\\
&+G_3)g(\xi_5(x_1,0),t)+(G_1+2G_2-2G_3)g(\xi_6(x_1,0),t)\\
&+(G_1-G_2+G_3)g(\xi_7(x_1,0),t)-3G_1g(\xi_8(x_1,0),t)\}.
\end{aligned}$$

Again, we can obtain the void nucleation time $t_{nuc,1}$ by solving the equation $\sigma_{1,T}(x_1, t_{nuc,1}) = \sigma_{crit}$. Fig. 6(a) demonstrates the stress distributions in the T-shaped tree shown in Fig. 3(b) that were obtained by COMSOL. Fig. 6(b) shows an evolution of the stress distributions across the wire segments 1 and 2 of the T-shaped tree that was obtained by COMSOL and the one-term approximation, which shows that the one-term approximation is very accurate.

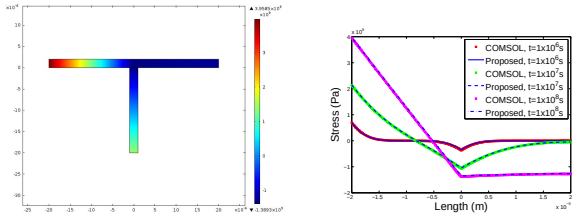

(a) (b)

Fig. 6. (a) The EM stress distribution in the T-shaped 4-terminal wires at the time $t = 1 \times 10^8 s$; (b) the EM stress development along the lines 1 and 2: $j_1 = 5 \times 10^{10} A/m^2$, $j_2 = 0 A/m^2$, $j_3 = 2.5 \times 10^{10} A/m^2$.

C. Cross-shaped 5-terminal interconnect tree

In the cross-shaped 5-terminal interconnect tree shown in Fig. 3(c), there are four segments which connect to each other through the middle contact "o". Again, the exact analytical solution of the stress evolution equation with the boundary and initial conditions corresponding to the void nucleation phase of this cross-shaped tree can be obtained. We only list the approximate solution using the first dominant term for the segment 1 of the cross-shaped tree:

$$\begin{aligned}\sigma_{1,+}(x_1,t) = -\frac{1}{4}\{&-4G_1 g(\xi_1(x_1,0),t) + (G_1 - G_2 + G_3 \\ &- G_4) g(\xi_2(x_1,0),t) + 2(G_1 + G_2 - G_3 + G_4) g(\xi_3(x_1,0),t) \\ &+ (G_1 - G_2 + G_3 - G_4) g(\xi_4(x_1,0),t)\} - \frac{1}{4}\{(G_1 - G_2 \\ &+ G_3 - G_4) g(\xi_5(x_1,0),t) + 2(G_1 + G_2 - G_3 + G_4) \\ &\times g(\xi_6(x_1,0),t) + (G_1 - G_2 + G_3 - G_4) g(\xi_7(x_1,0),t) \\ &- 4G_1 g(\xi_8(x_1,0),t)\}.\end{aligned}$$

Similarly, with σ_{crit} and the $\sigma_{1,+}(x_1, t)$, we can obtain the void nucleation time $t_{nuc,1}$ by solving the equation $\sigma_{1,+}(x_1, t_{nuc,1}) = \sigma_{crit}$.

As an illustration, we set the current densities in the four segments to $j_1 = 5 \times 10^{10} A/m^2$, $j_2 = 0 A/m^2$, $j_3 = 5 \times 10^{10} A/m^2$, and $j_4 = 10^{10} A/m^2$. We use COMSOL to simulate the stress distributions in the cross-shaped tree shown in Fig. 7(a). Again, the stress evolution from our model uses the one-term approximation and the results are shown in Fig. 7(b). It can be seen from Fig. 7 that the proposed one-term approximation solution matches the simulation results by COMSOL very well.

IV. Experimental Results and Discussions

The proposed dynamic EM model and analysis methods considering multi-branch interconnect trees have been implemented in Matlab and compared with COMSOL [23], which is considered golden in our work. The material parameters used in our numerical simulations are shown in Table I. The metal

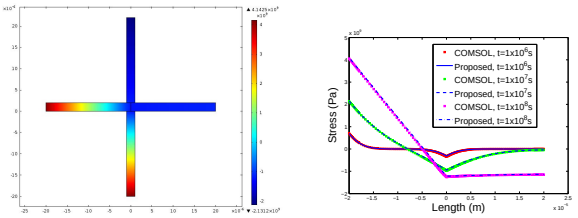

(a) (b)

Fig. 7. (a) The EM stress distribution in the cross-shaped 4-terminal interconnect tree at the time $t = 1 \times 10^8 s$; (b) the EM stress development along the lines 1 and 2: $j_1 = 5 \times 10^{10} A/m^2$, $j_2 = 0 A/m^2$, $j_3 = 5 \times 10^{10} A/m^2$, $j_4 = 10^{10} A/m^2$.

wire structures used in our experiment are shown in Fig. 3 and the length of each segment is set to $20 \mu m$.

A. EM model prediction with different current densities

We first study the EM model prediction against the results of COMSOL, using the one term ($n = 0$) approximation for the T-shaped 4-terminal interconnect tree. The EM stress distributions of the T-shaped wire structure (the segments 1 and 2 are shown here only) under different current density configurations are shown in Fig. 8(a)-(d). The stress profiles for different times are obtained from the one term approximation of the exact series solution. In the case (a), the stress distribution is similar to the 3-terminal single-wire case where the segment 1 (left) is the *reservoir* and the segment 2 (right) is the active *sink* with no zero current. Since $j_1 \gg j_2$, the hydrostatic stress in the segment 2 are all compressive (negative). For the case (b), the currents in the two segments have different directions. As a result, both of the segments (especially their cathode nodes) can see tensile stresses, which matches the results from COMSOL very well.

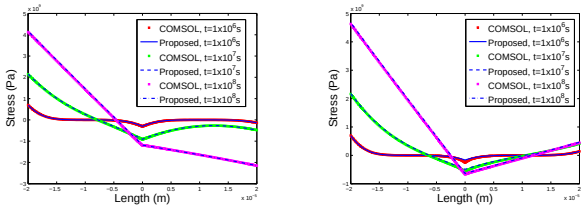

(a) $j_1 = 5 \times 10^{10} A/m^2$, $j_2 = 10^{10} A/m^2$, $j_3 = 2.5 \times 10^{10} A/m^2$ (b) $j_1 = 5 \times 10^{10} A/m^2$, $j_2 = -10^{10} A/m^2$, $j_3 = -2.5 \times 10^{10} A/m^2$

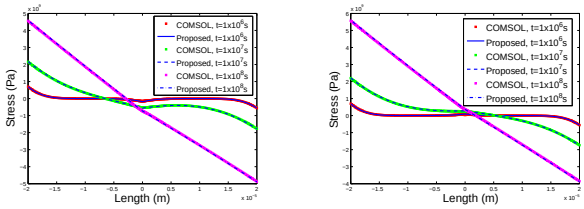

(c) $j_1 = 5 \times 10^{10} A/m^2$, $j_2 = 4 \times 10^{10} A/m^2$, $j_3 = 3 \times 10^{10} A/m^2$ (d) $j_1 = 5 \times 10^{10} A/m^2$, $j_2 = 4 \times 10^{10} A/m^2$, $j_3 = -3 \times 10^{10} A/m^2$

Fig. 8. The EM stress development along the lines 1 and 2 in the T-shaped 4-terminal interconnect tree.

B. Accuracy study for the compact EM models

Next, we study the accuracy of the EM models using different number of terms in the exact solution against the COMSOL results. Due to limited space, we only show the results for the straight-line 3-terminal interconnect case. We plot the relative errors against COMSOL using one item ($n = 0$), two items ($n = 1$), five items ($n = 4$) and ten items ($n = 9$), which are shown in Fig. 9(a)-(d), respectively. As we can see, by using just one item ($n = 0$), we can obtain relative errors less than 4%. By using two items ($n = 1$), the error is reduced to 0.5%. By using more terms ($n = 4$ and $n = 9$), the errors will stay around 0.5%, which means two items can achieve sufficient accuracy and adding a few more items will not increase the accuracy significantly. Such observations are also the case for all the tree interconnect types.

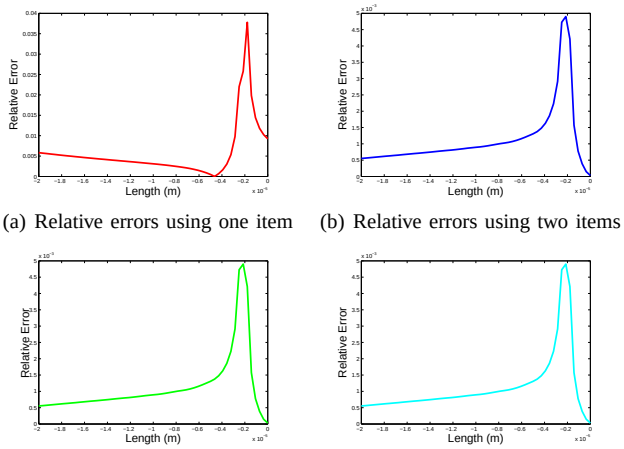

(a) Relative errors using one item (b) Relative errors using two items

(c) Relative errors using five items (d) Relative errors using ten items

Fig. 9. Relative errors between the proposed analytic model and the COMSOL model for the straight-line 3-terminal interconnect tree: $j_1 = 5\times10^{10}A/m^2$, $j_2 = 3\times10^{10}A/m^2$.

V. Conclusion

In this paper, we have proposed a new modeling and analysis technique for electromigration reliability analysis in multi-branch interconnect trees with continuous metallization, which reflects more practical VLSI interconnect structures and wiring techniques. We developed the exact analytic solutions to the stress evolution equations for the straight-line 3-terminal wires, the T-shaped 4-terminal wires, and the cross-shaped 5-terminal wires. The new physics-based EM models for multi-branch interconnect trees show an excellent agreement with the detailed numerical analysis. Experimental results showed that using the first dominant basis function can lead to less than 4 % errors. Furthermore, by using the first two basis functions, one can have less than 0.5% errors, which is sufficient for practical EM analysis.

References

[1] B. Bailey, "Thermally challenged," in *Semiconductor Engineering*, 2013.

[2] S. Chatterjee, M. B. Fawaz, and F. N. Najm, "Redundancy-Aware Electromigration Checking for Mesh Power Grids," in *IEEE/ACM International Conference on Computer-Aided Design (ICCAD)*, 2013.

[3] V. Mishra and S. S. Sapatnekar, "The Impact of Electromigration in Copper Interconnects on Power Grid Integrity," in *Design Automation Conference (DAC), 2013 50th ACM/EDAC/IEEE*, 2013.

[4] I. A. Blech, "Electromigration in thin aluminum films on titanium nitride," *Journal of Applied Physics*, vol. 47, no. 4, pp. 1203–1208, 1976.

[5] J. R. Black, "Electromigration-A Brief Survey and Some Recent Results," *IEEE Transactions on Electron Devices*, vol. 16, no. 4, pp. 338–347, 1969.

[6] M. Ohring, *Reliability and Failure of Electronic Materials and Devices - Milton Ohring - Google Books*. San Diego: Academic Press, 1998.

[7] J. R. Lloyd, "New models for interconnect failure in advanced IC technology," *Physical and Failure Analysis of Integrated Circuits, 2008. IPFA 2008. 15th International Symposium on the*, pp. 1–7, 2008.

[8] M. Hauschildt, C. Hennesthal, G. Talut, O. Aubel, M. Gall, K. B. Yeap, and E. Zschech, "Electromigration early failure void nucleation and growth phenomena in Cu and Cu(Mn) interconnects," in *2013 IEEE International Reliability Physics Symposium (IRPS)*, pp. 2C.1.1–2C.1.6, IEEE, 2013.

[9] M. Pathak, J. S. Pak, D. Pan, and S. K. Lim, "Electromigration modeling and full-chip reliability analysis for BEOL interconnect in TSV-based 3D ICs," in *Computer-Aided Design (ICCAD), 2011 IEEE/ACM International Conference on*, pp. 555–562, 2011.

[10] X. Huang, T. Yu, V. Sukharev, and S. X.-D. Tan, "Physics-based electromigration assessment for power grid networks," in *Proc. Design Automation Conf. (DAC)*, June 2014.

[11] V. Sukharev, "Beyond black's equation full-chip em/sm assessness in 3d ic stack," *Microelectronic Engineering*, vol. 120, pp. 99–105, May 2014.

[12] M. A. Korhonen, P. Borgesen, K. N. Tu, and C. Y. Li, "Stress Evolution Due to Electromigration in Confined Metal Lines," *Journal of Applied Physics*, vol. 73, no. 8, pp. 3790–3799, 1993.

[13] "Comsol multiphysics." http://www.comsol.com.

[14] S. P. Hau-Riege and C. V. Thompson, "Experimental characterization and modeling of the reliability of interconnect trees," *Journal of Applied Physics*, vol. 89, pp. 601–609, January 2001.

[15] A. V. Vairagar, S. G. Mhaisalkar, M. A. Meyer, E. Zschech, A. Krishnamoorthy, K. N. Tu, and A. M. Gusak, "Direct evidence of electromigration failure mechanism in dual-damascene cu interconnect tree structures," *Applied Physics Letters*, vol. 87, pp. 081909–1–081909–4, August 2005.

[16] C. Thompson, S. Hau-Riege, and V. Andleigh, "Modeling and experimental characterization of electromigration in interconnect trees," in *AIP Conference Proceedings*, 491, pp. 62–73, AIP Publishing, 1999.

[17] C. L. Gan, C. V. Thompson, K. L. Pey, and W. K. Choi, "Experimental characterization and modeling of the reliability of three-terminal dual-damascene cu interconnect trees," *Journal of Applied Physics*, vol. 94, pp. 1222–1228, July 2003.

[18] S. M. Alam, *Design Tool and Methodologies for Interconnect Reliability Analysis in Integrated Circuits*. PhD thesis, Massachusetts Institute of Technology, September 2004.

[19] S. P. Hau-Riege and C. V. Thompson, "Electromigration saturation in a simple interconnect tree," *Journal of Applied Physics*, vol. 88, pp. 2382–2385, September 2000.

[20] S. Hau-Riege, *New Methodologies for Interconnect Reliability Assessments of Integrated Circuits*. PhD thesis, Massachusetts Institute of Technology, June 2000.

[21] J. J. Clement, S. P. Riege, R. Cvijetic, and C. V. Thompson, "Methodology for Electromigration Critical Threshold Design Rule Evaluation," *IEEE Trans. on Computer-aid Design of Integrated Circuits and Systems*, vol. 18, no. 5, pp. 576–581, 1999.

[22] M. Lin and A. Oates, "An Electromigration Failure Distribution Model for Short-Length Conductors Incorporating Passive Sinks/Reservoirs," *IEEE Transactions on Device and Materials Reliability*, vol. 13, pp. 322–326, March 2013.

[23] www.comsol.com, "COMSOL Mutiphysics: User Guide," *Version 4.1*.